HHS Public Access

Author manuscript

J Immunol. Author manuscript; available in PMC 2016 October 01.

Published in final edited form as:

J Immunol. 2015 October 1; 195(7): 3086–3099. doi:10.4049/jimmunol.1500610.

Female-specific down-regulation of tissue-PMN drives impaired Treg and amplified effector T cell responses in autoimmune dry eye disease[1]

Yuan Gao[*], **Kyungji Min**[*], **Yibing Zhang**[*], **John Su**[*], **Matthew Greenwood**[*], and **Karsten Gronert**[*]

[*]Vision Science Program, School of Optometry, University of California Berkeley

Abstract

Immune-driven dry eye disease primarily affects women; the cause for this sex-specific prevalence is unknown. PMN have distinct phenotypes that drive inflammation but also regulate lymphocytes and are the rate-limiting cell for generating anti-inflammatory lipoxin A_4 (LXA_4). Estrogen regulates the LXA_4 circuit to induce delayed female-specific wound healing in the cornea. However, the role of PMN in dry eye disease remains unexplored. We discovered a LXA_4-producing tissue-PMN population in the corneal limbus, lacrimal glands and cervical lymph nodes of healthy male and female mice. These tissue-PMN, unlike inflammatory-PMN, expressed a highly amplified LXA_4 circuit and were sex-specifically regulated during immune-driven dry eye disease. Desiccating stress in females, unlike in males, triggered a remarkable decrease in lymph node PMN and LXA_4 formation that remained depressed during dry eye disease. Depressed lymph node PMN and LXA_4 in females correlated with an increase in T effector cells (T_H1 and T_H17), a decrease in regulatory T cells (T_{reg}) and increased dry eye pathogenesis. Antibody depletion of tissue-PMN abrogated LXA_4 formation in lymph nodes, caused a marked increase in T_H1 and T_H17 and decrease in T_{reg} cells. To establish an immune regulatory role for PMN-derived LXA_4 in dry eye females were treated with LXA_4. LXA_4 treatment markedly inhibited T_H1 and T_H17 and amplified T_{reg} cells in draining lymph nodes, while reducing dry eye pathogenesis. These results identify female-specific regulation of LXA_4-producing tissue-PMN as a potential key factor in aberrant T effector cell activation and initiation of immune-driven dry eye disease.

Keywords

Dry Eye disease; PMN; Lipoxin A_4; sex-specific; T_H1; T_H17; T_{reg}; lymph node

Introduction

The concept of PMN's single-track fate as terminally differentiated and short-lived primary effector cells of host defense and acute inflammation is rapidly evolving. PMN are the most

[1]Vision Science Program, School of Optometry, University of California Berkeley, Berkeley, CA 94720

Address correspondence to Dr. Karsten Gronert, Vision Science Program, School of Optometry, University of California Berkeley, 594 Minor Hall, MC 2020, Berkeley, CA 94720-2020, Phone: 510.642.1076, kgronert@berkeley.edu.

The authors have declared that no conflict of interest exists.

abundant effector leukocytes in the innate immune system and recent discoveries have dramatically expanded their function from simply killing pathogens to regulating innate and adaptive immune responses (1–6). Compelling evidence has defined distinct PMN phenotypes that have immune-regulatory and -suppressive functions. Non-traditional functions for PMN have been reported in the ocular surface where innate and adaptive immune responses are tightly regulated to preserve the delicate visual axis. Unlike their paradigm pro-inflammatory role, PMN in the cornea are critical for wound healing of minor epithelial injuries and drive nerve regeneration (7–11). These unexpected roles of PMN in corneal inflammatory/reparative responses have been attributed in part to their key role in generating specialized pro-resolving mediators (SPM) of which the eicosanoid lipoxin A_4 (LXA_4) is the most abundant. This SPM has wide-ranging anti-inflammatory, wound healing actions and promote clearance of apoptotic PMN by macrophages in acute inflammatory responses (12).

Peripheral blood PMN highly express the conserved 5-lipoxygenase, 5-LOX, that is the rate limiting enzyme for generating leukotriene B_4 (13), an eicosanoid that amplifies host defense and recruits and controls effector T cells (14, 15). The diverse role of PMN is underscored by the fact that 5-LOX is also the rate-limiting enzyme for LXA_4 formation. In tissues, LXA_4 synthesis requires the coordinated interaction of two enzymes 5-LOX and 15-LOX, which are both expressed in mouse PMN and in humans can be induced to switch function of recruited peripheral blood PMN from host defense to resolving acute inflammation (12, 16, 17). Hence, depending on the state of activation or potentially phenotype, PMN can either amplify or resolve acute inflammation (16). Limited studies have investigated if the SPM LXA_4, like its pro-inflammatory counterpart LTB_4, has direct actions on T cells (18). However, several reports have demonstrated interactions of PMN with B- and T-lymphocytes and PMN regulation of lymphocyte function (2–5); hence, PMN are ideally situated as regulatory cells at the interphase of innate and adaptive immune responses.

Due to the normal immune privileged state of the cornea, the ocular surface has been studied extensively as a model to understand regulation and suppression of effector T cell activation. An immune-driven ocular disease, whose pathogenesis is initiated by disrupting suppression of effector T cell activation, is aqueous tear deficient dry eye disease, which is one of the most frequent ocular morbidities (19–21). Key features of the pathogenesis is activation and homing of effector T cells to the lacrimal gland, conjunctival goblet cells and cornea, which initiates chronic inflammation and epithelial defects that can lead to blindness. Treatment options currently are limited to artificial tears, corticosteroids and the immunosuppressant cyclosporine A. The etiology of this common ocular immune disease is unknown or the cause for its striking prevalence in women (22, 23). We recently reported on marked sex-specific differences in corneal inflammatory/reparative responses in both humans and mice (24, 25). More importantly, we identified estrogen downregulation of the resident corneal LXA_4 circuit as a mechanism for the female phenotype of delayed epithelial wound healing and altered PMN functional responses (24).

The aim of this study was to determine if PMN and LXA_4 have a role in sex-specific dry eye pathogenesis, which has not been investigated. Here we report on a tissue population of

PMN in normal draining lymph nodes, lacrimal glands and the limbus of the cornea. These resident tissue-PMN express a highly amplified LXA_4 pathway and generated LXA_4 in draining lymph nodes. A striking sex-specific difference was that desiccating stress triggered downregulation of the tissue-PMNL-LXA_4 circuit selectively in females, which induced amplified effector T cell activation. More importantly, we were able to recapitulate this female-specific dry eye response by depleting LXA_4 producing tissue-PMN, which provides evidence for a potential key checkpoint system for maintaining appropriate Treg function and preventing aberrant activation of T_H1 and T_H17 cells in females.

Materials and Methods

Animals

Age- matched (6- to 10-wk-old) C57BL/6J female and male mice were purchased from Jackson Laboratory (Bar Harbor, ME, USA). Mice were housed on a 12-hour day/night cycle and fed a standard diet ad libitum (rat/mouse diet LM-485; Harlan Tekland, Madison, WI, USA). All animal studies have been approved by the University of California Berkeley Animal Care and Use Committee, and performed according to the U.S. National Institutes of Health (NIH) Guide for the Care and Use of Laboratory Animals.

Aqueous tear deficient dry eye mouse model

The standard model of desiccating environmental stress was used to induce immune-driven dry eye disease (20, 26–28). Briefly, mice were placed in cages with a perforated screen walls and exposed to continuous airflow from fans in a low humidity (20–30%) cubicle. Lacrimal gland function was inhibited by injection with scopolamine hydrobromide (0.1 mL of 10 mg/mL, formulated in sterile saline; Sigma-Aldrich Corp., St Louis, MO) for 3 or 5 consecutive days, and a reduced dose (0.1 mL of 5 mg/mL) for 10 days, respectively. Scopolamine hydrobromide injections were performed three times per day (9 AM, 2 PM, and 7 PM), subcutaneously into alternating hindquarters of mice. Age- and sex-matched untreated mice housed in standard animal facility environment served as healthy controls. In selected experiments mice were rendered neutropenic (29, 30) by *i.p.* injection of purified anti-Ly6g (1A8 clone, 200 μg, BD PharMingen) 24 h prior to starting desiccating stress (1^{st} injection) and 2 days after induction of dry eye disease (2^{nd} injection). Control mice received the same dose of serum type IgG. Selected mice were treated topically (100 ng, *tid*) and systemically (1 μg, *qd*) with LXA_4 (Cayman Chemical, Ann Arbor, MI) or sterile saline alone (PBS, ph 7.4) throughout 10 days of desiccating stress. Ethanol from LXA_4 stock solution was rapidly removed under gentle stream of nitrogen and autacoids immediately resuspended in sterile saline and applied to the eye (5μl/drop) (31, 32). Corneas with complete limbus, lacrimal glands and cervical draining lymph nodes were surgical excised with sterile instruments, and cleaned in ice-cold sterile phosphate-buffered saline under a dissecting microscope. Lacrimal glands were weighed and each draining lymph node was extracted with the diameter controlled 1.8–2.0 mm. Isolated tissues were either snap frozen for RNA/lipidomic/myeloperoxidase analyses or immediately processed for flow cytometry/ immunohistochemistry.

Dry eye disease assessment

Clinical signs of dry eye were assessed by corneal fluorescein staining (CFS) using 0.5 μL of 2.5% Fluorescein Sodium (Bausch & Lomb) in accordance with the standard National Eye Institute scoring system(33, 34). Tear production was measured by the cotton thread test (CTT). Briefly, a phenol red thread (Zone-Quick; Showa Yakuhin Kako Co., Tokyo, Japan) was placed in the lateral canthus of the conjunctiva fornix of each eye for 30 seconds after excess tear had been removed for a standard time of 30 seconds, and tear distance (in millimeters) was read under a microscope (Carl Zeiss, Jena, Germany).

PMN and lymphocyte isolation

Tissue-PMN were isolated from lacrimal gland and cervical lymph nodes of normal female mice. Naïve T cells and activated $CD4^+$ T cells were isolated from cervical draining lymph nodes. Briefly, the tissues were minced and filtered through a 40-μm cell strainer (BD Falcon; BD Bioscience, Inc., San Diego, CA). After preparing a single-cell suspension, cells were negatively separated and isolated by using neutrophil/$CD4^+$ T cell isolation kits (Miltenyi Biotec, Bergisch-Gladbach, Germany) according to the manufacturer's instructions. Inflammatory PMN were collected from zymosan A induced peritonitis exudates in C57BL/6 female mice. Briefly, normal female mice were injected *i.p.* with 1 mg zymosan A (Sigma, St. Louis, MO, USA) in 1 mL sterile HBSS. After 12 h, which is the peak of PMN infiltration in this model (35), peritoneal lavages that contain >90% PMN were collected with sterile HBSS. Cells were stained with Trypan blue and counted using light microscopy. The cell suspension was pelleted by centrifugation followed by washing in RPMI 1640 with 5% FBS. Cell pellet was re-suspended (5×10^5 PMN/ml) in 200μL RPMI 1640 with 5% FBS either for histological analysis, or were activated with calcium ionophore (37°C, 15 min, 5μM) to establish endogenous lipid mediator formation.

Histological sections

Whole eyes and lymph nodes were removed and embedded in optimal cutting temperature (OCT) compound (Sakura Finetek, Torrance, CA, USA). The samples were then allowed to set at −80°C for ≥2h before being cross-sectioned lengthwise into 5-μm-thick slices. Conventional smears on slides were prepared from isolated neutrophils. Sections and smears were stained with Hematoxylin and eosin (H&E) for evaluating morphology to distinguish cell types.

Periodic Acid-Schiff (PAS) staining

Sections of whole eyes were processed according to conventional histologic techniques for Periodic Acid-Schiff (PAS) staining. Briefly, histological sections were fixed in 4% paraformaldehyde, oxidized in 100 μL of 0.5% periodic acid solution and treated with 100 μL of Schiff reagent. After computer capture through a 10x magnification setting via light microscopy (Carl Zeiss, Jena, Germany), goblet cell numbers were manually counted and mucin area were assessed through ImageJ software by calculating area and density through intensity-threshold settings.

Immunofluorescence and deconvolution imaging

Immunofluorescence and deconvolution imaging was performed as described previously (36). In brief, corneas with complete limbus were fixed (2% formaldehyde), permeabilized (0.1% Triton X-100), and then incubated with the following fluorescence-labeled mAb: FITC- or PE-conjugated anti-Ly6g (1A8 clone; BD PharMingen, San Diego, CA, USA) for PMN; FITC- or PE-conjugated anti-CD31 (MEC 13.3 clone; BD PharMingen) for limbal vessel endothelium; PE-conjugated anti-CD3 (500A2 clone; BD PharMingen) for T cells; FITC- or APC- conjugated anti-CD4 (RM4-5 clone; BD PharMingen) for activated $CD4^+$ T cells. Each step was followed by three washes with PBS. Controls using isotype- and species- matched antibodies were in all cases negative. Radial cuts were made in the cornea so that it could be flattened under a coverslip, and the cornea was mounted in Celvol (Sekisui Specialty Chemical Company, Dallas, TX, USA), containing 1 μg/ml DAPI (Sigma-Aldrich, St. Louis, MO, USA), to assess nuclear morphology. Image analysis and quantification of corneas were performed using DeltaVision Elite deconvolution microscope (Applied Precision, Issaquah, WA, USA). Whole mounts were evaluated using a 40X oil immersion lens to assess each field of view across the diameter of the cornea (from limbus to limbus). Each field of view has a tissue diameter of 0.53 mm. The limbal region encompasses the limbal vessels and the remaining regions include the avascular cornea. The graphical values were obtained by counting the total number throughout the depth of the cornea from the epithelial to endothelial surfaces (a range of ~90μm) in each of nine, 40X fields of view comprising the diameter of a cornea (9, 36).

Myeloperoxidase (MPO) assay

PMN were quantified in lacrimal glands and lymph nodes at indicated time points by measuring MPO activity, as a specific and quantitative index of tissue PMN infiltration (7, 31, 32). In brief, tissues were homogenized in 450 μl of 50 mM potassium phosphate buffer containing 0.5% hexadecyltrimethylammonium bromide (pH 6.0), followed by sonication, circles of freeze-thaw. After centrifugation, MPO activity in supernatants was measured by spectrophotometry using o-dianisidine dihydrochloride oxidation as a colorimetric indicator. Calibration curves for conversion of MPO activity to PMN number were established with PMN collected from zymosan A-induced peritonitis in C57BL/6J mice.

Flow cytometry analysis

Lacrimal glands were digested with 2mg/mL collagenase D (Roche Diagnostic Corp.) and 0.5 mg/mL DNase I (Roche Diagnostic Corp.) in FCS-containing RPMI for 1 h at 37°C. Single-cell suspensions from the digested samples and draining lymph nodes were prepared with a 40-μm cell strainer (BD Falcon; Becton-Dickinson, Franklin Lakes, NJ). Fc receptors were blocked with anti-FcR mAb (BD PharMingen, San Diego, CA) and cells were then incubated with titrated amounts of fluorescent-labeled antibodies: FITC- conjugated anti-Ly6g (1A8 clone; BD PharMingen, San Diego, CA, USA) for PMN; PE-conjugated anti-CD45 (MEC 13.3 clone; BD PharMingen) for leukocytes; PE-conjugated anti-CD3 (500A2 clone; BD PharMingen) for T cells; FITC- conjugated anti-CD4 (RM4-5 clone; BD PharMingen) for activated $CD4^+$ T cells; APC- conjugated anti-IFN-γ (XMG1.2; TONBO biosciences); FITC- or APC conjugated anti-IL17 (eBio17B7; ebioscience); APC-

conjugated anti-Foxp3 (3G3; TONBO biosciences). Isotype control was stained with the appropriately matched antibodies. Data were analyzed with FlowJo (TreeStar, Ashland, OR, USA) software. The percentage of stained cells in the samples was calculated with respect to isotype control staining. Cell sorting was performed using a high-speed cell sorter (MoFlo, SX DakoCytomation, Inc., Fort Collins, CO, USA). Each flow cytometry experiment was performed at least three times.

Analysis of gene expression

RNA from neutrophils, naïve T cells and $CD4^+$ T cells was isolated using RNA Easy Mini Kit (Qiagen Sciences, Germantown, MD, USA) and quantified by spectrophotometry. RNA was then reverse transcribed using a High-Capacity cDNA Kit (Applied Biosystems, Foster City, CA, USA). β-Actin was used as a reference gene. Real-time PCR was performed using SYBR Green Master Mix (Applied Biosystem) with a StepOne Plus qPCR system (Applied Biosystems) as described previously (24, 32, 37). Amplifications were run in duplicates and efficiency curves for all primers (supplement table 1) were established. Comparative quantification of gene expression was performed by StepOne software (Applied Biosystems). Relative expression was expressed as fold change from a mouse reference universal RNA control that was generated by pooling mRNA from C57BL/6J mouse spleen and kidney.

Lipid mediators analysis

LC/MS/MS-based lipidomic analysis was used to identify and quantify lipid mediators as previously described (32, 37–39). Class specific deuterated internal standards (PGE_2-d4, LTB_4-d4, 15-HETE-d8, LXA_4-d5, DHA-d5, AA-d8) were used to calculate work up and extraction recovery. LC/MS/MS system consisting of an Agilent 1200 Series HPLC, Shiseido Capcell Pak C18 column, and AB Sciex QTRAP 3200 MS. Mobile phases used were A: 71.9% water/28% acetonitrile/0.1% acetic acid (vol/vol/vol) and B: 60% isopropanol/40% acetonitrile (vol/vol) that was run as a gradient. MS/MS analyses were conducted in negative ion mode, and lipids were quantitated using scheduled multiple reaction monitoring (MRM) mode using specific and established transition ions. Calibration curves were prepared from synthetic standards (Cayman Chemical Company).

Statistical analysis

All data are presented as mean ± SEM. One-tailed, unpaired Student's *t* test was used to evaluate the significance of differences between two sex-specific groups. One-way ANOVA with Tukey's post hoc testing was used for overall statistical comparisons. $P < 0.05$ was considered statistically significant. These tests were performed with GraphPad Prism software (GraphPad Inc., San Diego, CA) and SigmaPlot (Systat Software, San Jose, CA).

Results

Desiccating stress causes increased ocular surface pathogenesis in females

Due to the female prevalence of dry eye in humans, all dry eye animal models are carried out in females. However, no studies have investigated if dry eye disease pathogenesis in animal models or humans exhibits sex-specific differences. A key feature of advanced

aqueous tear deficient dry eye is damage to the corneal epithelial layer. Hence, we investigated if dry eye induces sex-specific ocular surface pathogenesis if matched male and female mice are exposed to the standard mouse model of aqueous tear deficient dry eye disease (19, 26, 28). Desiccating stress induced significantly greater epithelial defect in females at 3 days and 5 days when directly compared to males using a standard clinical fluorescent scoring method (Fig. 1A). Extended desiccating stress eventually led to identical and marked increase in epithelial defect after 10 days in both males and females. Epithelial defect correlated with sex-specific decrease in tear production in response to desiccating stress evidenced by significantly lower tear production in females 3–10 days compared to males (Fig. 1B). Another feature of this mucosal immune disease is loss of goblet cells in the conjunctiva. Conjunctival goblet cells (Fig 1C) were counted manually, and total mucin area was quantified in eyelids of females and males as a marker of mucin secretion. Healthy male mice had a significantly higher number of goblet cells compared to females, whereas no significant sex-specific differences were observed in total mucin area in the healthy conjunctiva. Desiccating stress reduced goblet cell numbers in both males and females after 10 days of dry eye. Consistent with sex-specific differences in corneal epithelial defects desiccating stress also induced a greater decrease in the number of goblet cells and a 49 ± 11% greater decrease in mucin production in females versus males (Fig 1C).

Sex-specific regulation of a tissue PMN population and effector CD4$^+$ T cell activation in the corneal limbus

Using a combined approach of immunohistochemistry (IHC) and flow cytometry, we next assessed the presence of PMN in uninjured corneas and during desiccating stress (3-10 days) in both males and females. IHC confirmed no significant or consistent PMN presence in healthy corneas or stressed corneas at any of the time points. However, we detected a population of CD45 (a pan leukocyte marker) and Ly6g (a selective PMN marker) positive cells that exhibited the morphology and characteristic polymorphonuclear shape of PMN in the corneal limbal region of healthy uninjured eyes (Fig. 2A-D). This small but significant population of tissue PMN was located near but not in blood vessels throughout the limbus (Fig. 2C). Quantification by manual cell counting in a defined whole mount grid (Fig. 2C) and flow cytometry analysis (Fig. 2D) established the presence of this basal tissue-PMN population in healthy male and female eyes with no sex specific differences. Unexpectedly, desiccating stress, which is a well-defined trigger for ocular surface inflammation and immune responses, induced a marked decrease in the tissue-PMN population at the corneal limbus. More importantly, this decrease was significantly amplified in females (70 ± 4 %) compared to males (49 ± 4%) at 3 days and tissue PMN level remained depressed 3 – 10 days based on analysis by IHC (Fig. 2B, C). Analysis of the cornea with attached limbus by flow cytometry confirmed and was consistent with limbus-alone IHC results (Fig. 2D), except at 10 days where flow cytometry did not detect a sex specific difference.

Activation of effector T cells and the subsequent targeting of CD4$^+$ T cells to the ocular surface and lacrimal gland is a key feature of immune pathology in human autoimmune dry eye disease and the desiccating stress mouse model (20, 26, 27). A low number of CD4$^+$ T cells were present in the limbus of healthy eyes in both males and females and their numbers increased with duration of desiccating stress with a sharp increase (10–15 fold) in CD4$^+$ T

cells after 10 days (Fig. 2E, F). IHC and flow cytometry analysis both documented a marked sex-specific difference in the number of activated $CD4^+$ T cells that was 64 ± 22% and 70 ± 17% higher, respectively, in females when directly compared to males at 10 days. Analysis by flow cytometry captured and measured T cell populations in both cornea and limbus. The analysis established a continuous increase in $CD4^+$ T cells from 3 days to 10 days and higher levels of $CD4^+$ T cell in healthy/uninjured corneas of females and at every time point during desiccating stress when directly compared to matched males (Fig. 2F).

Desiccating stress triggers an amplified PMN and $CD4^+$ T cells response in female lacrimal glands

Ocular surface and lacrimal gland function as an integrated unit linked by sensory and autonomic nerves and the tear film. The lacrimal gland is a primary target for immune driven dry eye disease in humans and mice (19, 20, 27). Hence, we investigated if desiccating stress induces sex-specific $CD4^+$ T cell activation and if PMN are presented in the lacrimal glands during the dry eye disease time course. Lacrimal glands from matched healthy males and females both contained significant number of PMN ($CD45^{high}$, $Ly6g^{high}$) whose identity were established by flow cytometry (Fig. 3A) and confirmed by myeloperoxidase (MPO) activity (Fig. 3B), a specific enzymatic marker of PMN. Lacrimal glands from females contained 161% higher levels of tissue PMN (78,269 ± 20,812) compared to males. Desiccating Stress triggered a pronounced and early influx of PMN (159,878 ± 25,862) into lacrimal glands of females as evidenced by a 2-fold increase in lacrimal gland PMN at day 3. The PMN response to desiccating stress in females was 1.57-fold higher than the PMN response (101,1878 ± 17, 958) in males at day 3. Except at day 10, female mice consistently had significantly higher number of PMN in lacrimal glands throughout the time course of dry eye disease. Both females and males had low but significant levels of naïve T cells ($CD3^{high}$) and activated $CD3^{high}$, $CD4^{high}$ T cells in healthy unstressed lacrimal glands (Fig. 3C). Coincident with elevated levels of tissue PMN, the lacrimal glands of females also contained higher numbers of activated $CD4^+$ T cells. Consistent with the pathogenesis of immune driven dry eye disease, desiccating stress triggered a marked increase in lacrimal gland $CD4^+$ T cells. Activation of T cells was amplified in females early in the time course (3 days) and at the peak of dry eye disease (10 days), evidenced by 53 ± 19% and 69 ± 18% higher numbers of $CD4^+$ T cells in females, respectively, when directly compared to males.

Endogenous and sex-specific formation of LXA_4 and PGE_2 in healthy and stressed lacrimal glands

Formation of eicosanoids or LXA_4 in lacrimal glands has not been determined but the high number of tissue-PMN in the lacrimal gland sets in place a prominent resident biosynthetic route. LC/MS/MS-based lipidomic analysis demonstrated endogenous and high levels of LXA_4 formation (Fig. 3D) in healthy lacrimal glands and during the time course of dry eye disease in females (0.74 – 2.39 ng/10 mg) and males (0.44 – 1.21 ng/10 mg). Levels of LXA_4 formation (Fig. 3D) correlated with sex-specific difference in lacrimal gland PMN content (Fig. 3A-B) and accordingly LXA_4 levels were markedly higher in females than in males in both uninjured lacrimal glands and during desiccating stress (3 – 5 days). Both LXA_4 formation and PMN number in the lacrimal gland peaked 3 days after initiating dry

eye disease in females. Lipidomic analysis also demonstrated higher basal levels of PGE_2 (Fig. 3E) in the healthy lacrimal gland of females (179 ± 71 pg in females versus 46 ± 9 pg in males) and marked induction (3.4 fold) of PGE_2 formation in females at 3 days. PGE_2 is a pleiotropic regulator of inflammatory/immune responses and in both males and females, its level remained elevated 3–5 days after initiating dry eye disease and returned to baseline by 10 days.

Female-specific regulation of resident PMN and T cell activation in cervical draining lymph nodes

Cervical lymph nodes, which drain the head region, including the eyes, are critical sites for the induction of ocular surface immune responses, i.e. effector T cell activation. The presence or role for a PMN - LXA_4 circuit in lymph nodes has not been explored, even though crosstalk of PMN - T cells (2-4) has emerged as an important new concept and direct regulation of T cell function by LXA_4 has been reported (18, 40). Routine IHC analysis identified a population of $Ly6g^+$ polymorphonuclear cells in cervical draining lymph nodes of healthy and normal male and female mice (Fig. 4A). PMN morphology of these cells was confirmed by H&E staining of lymph node sections (Fig. 4B). For further identification, lymph node PMN were isolated by a magnetic cell separation and isolation system or FACS. The isolated lymph node PMN expressed $CD45^{high}Ly6g^{high}$ and demonstrated characteristic PMN morphology (Fig. 4C). In order to quantify changes in lymph node PMN numbers, we employed two independent approaches using both established surface markers and selective antibodies (CD45, Ly6g) for flow cytometry analysis and MPO assay as a PMN selective enzymatic marker. Flow cytometry and MPO analysis documented equivalent results (Fig. 4D, E). PMN content in cervical draining lymph nodes from healthy female mice was 4.2 ± 0.3 and 1.8 ± 0.1 fold higher than in matched males based on MPO and flow cytometry quantification, respectively.

Desiccating stress triggered a marked increase in lymph node PMN in males that peaked at 3 days and demonstrated 10.7 ± 0.2 and 2 .1 ± 0.1 fold increase over baseline measured by MPO assay and flow cytometry, respectively. A striking female-specific response to desiccating stress was marked decrease in lymph node PMN by 64 ± 7% and 76 ± 2 % as measured by MPO and flow cytometry analysis, respectively. In sharp contrast, in male lymph nodes, PMN number remained significantly elevated throughout the desiccating stress, while in female lymph nodes PMN levels remained depressed and failed to return to baseline. Desiccating stress is a mouse model of immune-driven dry eye diseases (19, 20, 26) and consistent with the model $CD4^+$ T cells increased in draining lymph nodes in both males and females, which was assessed by flow cytometry analysis (Fig. 4F). However, in males a significant increase in $CD4^+$ T cells was not observed until day 10 while in females $CD4^+$ T cells increased significantly as early as day 3. The magnitude of $CD4^+$ T cell activation in female lymph nodes was 48 – 94% higher at all time points when directly compared to matched males. Coincident with the 64 ± 1 % drop in tissue PMN in female lymph nodes $CD4^+$ T cell also increased by 80 ± 2 % as early as 3 days after initiating dry eye disease (Fig. 4E, F). By contrast, in males, lymph nodes PMN levels peaked at 3 days and there was no change in $CD4^+$ T cell numbers compared to baseline.

Sex-specific regulation of effector T_H1, T_H17 cells and regulatory T cells (T_{reg}) activation in cervical draining lymph nodes

$CD4^+$ T cells, include autoreactive IFN-γ producing T_H1 and IL-17 producing T_H17 effector T cells as well as T_{reg} that suppress T effector cell activation. Dysregulation of T_H1 and T_H17 effector cells and impaired T_{reg} function have been implicated in driving immune pathogenesis in dry eye disease (41–45). Hence, we sought to determine if desiccating stress induces sex-specific effector T cell activation, and T_{reg} responses. Analysis by flow cytometry documented a marked sex-specific difference in the number of T_H1 (Fig. 5B) and T_H17 cells (Fig. 5C) that was 206 ± 41% and 89±7% higher, respectively, in females when directly compared to males. Desiccating stress also induced a "26 ± 1%" decrease in T_{reg} (Fig. 5A) in female lymph nodes. In sharp contrast, in males, T_{reg} cells level increased by 31 ± 8% compared to baseline, which directly correlate with a lower amplitude of effector T cell activation.

Female-specific changes in the lymph node PMN-LXA_4 circuit during desiccating stress

Dependent on the state of activation, PMN are a rate-limiting factor for LXA_4 formation at sites of innate immune responses. Hence, we assessed if LXA_4 is formed in draining lymph nodes and how it correlates with tissue-PMN content in females. Lipidomic analysis (Fig. 6A) established endogenous formation of LXA_4 as well as biosynthetic pathways markers for 5-LOX and 15-LOX, namely 5-HETE and 15-HETE, respectively. 5-LOX and 15-LOX synthesis of LXA_4 is the primary pathway for LXA_4 formation in tissues. During the coordinated synthesis the 15-LOX product 15-HETE is a substrate for 5-LOX, which converts 15-HETE to LXA_4. LXA_4 levels and 5-LOX and 15-LOX activity in lymph nodes of healthy and uninjured females was 2.8 – 5.0 fold higher (Fig. 6B) compared to males. The amplified LXA_4 pathway in females correlated with a 2–3 fold higher number of PMN in female lymph nodes when directly compared to males (Fig. 6C). Desiccating stress abrogated LXA_4 formation starting at day 3 in lymph nodes of females (Fig. 6B). Abrogated LXA_4 formation in females correlated with a marked decrease in basal lymph node PMN content in females (Fig. 6C) and decreased levels of biosynthetic pathway markers, 5-HETE and 15-HETE (Fig. 6B). In sharp contrast, 5-HETE and 15-HETE levels peaked at day 3 in lymph nodes from males, which correlates with the peak of PMN infiltration in male lymph nodes. Independent of PMN levels, LXA_4 formation decreased with induction of desiccating stress in male lymph nodes. PGE_2, a prostaglandin with pleiotropic inflammatory and immune regulatory action, was formed in lymph nodes of healthy uninjured males and females. PGE_2 levels markedly increased and peaked at 3 and 5 days in males and females, respectively. Analysis of lymph node PMN content and LXA_4 levels revealed a direct correlation that suggested PMN dependent formation of LXA_4 in female lymph nodes (Fig. 6C), which also was observed in female lacrimal glands (Fig. 6D).

Depletion of Tissue PMN amplifies CD4 T cell activation and dry eye pathogenesis

In order to assess if tissue PMN in corneal limbus, lacrimal gland and cervical lymph nodes impact immune pathogenesis of dry eye in females, namely effector $CD4^+$ T cell activation, we used an antibody approach to globally deplete PMN (10, 30, 46). In order to ensure sustained neutropenia and to capture early immune activation we selected 3 days of

desiccating stress as the time point for these experiments. Peritoneal injection of a specific and established Ly6g monoclonal (1A8) antibody reduced tissue PMN content (Fig. 7A-C) by 64% ± 5%, 90 ± 6% and 52 ± 8% in the limbus, lacrimal gland and cervical lymph node, respectively. Tissue neutropenia inversely correlated with a marked increase in effector $CD4^+$ T cells that increased by 277 ± 84%, 97 ± 19% and 53 ± 17% in the corneal limbus, lacrimal gland and cervical lymph nodes, respectively, indicating that tissue PMN are a determinant for $CD4^+$ T cell activation in the ocular surface. We next determined if PMN depletion impacts ocular surface pathogenesis. Consistent with an amplified $CD4^+$ T cell response tissue neutropenia markedly increased dry eye induced corneal defects by 75 ± 13% (Fig 7D) and significantly decreased conjunctiva goblet cell numbers in females (Fig S1).

Depletion of tissue-PMN in females amplifies effector T_H1 and T_H17 activation and downregulates T_{reg} cells

Since tissue neutropenia correlates with a marked expansion of $CD4^+$ T cells in draining lymph nodes, we determined the differential effect of PMN depletion on T_H1, T_H17 and T_{reg} populations in dry eye diseases. Tissue neutropenia caused a marked increase 123 ± 10% increase in T_H1 (Fig. 8B) and a 32 ± 5% increase in T_H17 (Fig. 8C) effector T cells in the draining lymph nodes when compared to control females that were subjected to 10 days of desiccating stress. The amplified T_H1 and T_H17 response in neutropenic mice correlated with a 26 ± 5% decrease in regulatory T cells in draining lymph (Fig. 8A). Taken together, these findings identify a previously unknown function for PMN in regulating effector T cell responses triggered by ocular surface desiccating stress.

Depletion of tissue-PMN in females impairs LXA_4 formation in lymph nodes and lacrimal glands

To determine if PMN depletion and subsequent increased $CD4^+$ T cell activation correlates with impaired tissue LXA_4 formation, we carried out lipidomic analysis of lacrimal gland and cervical lymph nodes as they are the primary sites for effector $CD4^+$ T cell targeting and/or activation in aqueous tear deficient dry eye disease. Three days of desiccating stress was selected for the lacrimal gland and 0 day (uninjured/healthy) was selected for lymph nodes as these time points in females represent the peak PMN content in these two tissues. Consistent with our hypothesis, PMN depletion caused a 41 ± 13 % decrease in LXA_4 formation in the lacrimal gland as well as the LXA_4 and PMN biosynthetic pathway markers, 5-HETE (5-LOX) and 15-HETE (15-LOX) (Fig. 9A). In the draining lymph nodes PMN depletion completely abrogated LXA_4 formation and significantly decreased 5-HETE and 15-HETE levels by 37 ± 14 % and 64 ± 14 %, respectively (Fig. 9B). In contrast, PMN depletion did not significantly change PGE_2 levels in female lymph nodes.

Tissue-PMN express an amplified LXA_4 circuit that regulates T_H1, T_H17 and T_{reg} cells in lymph nodes

To determine if isolated tissue-PMN have the capacity to generate LXA_4, we isolated PMN from draining lymph nodes and lacrimal glands of normal, healthy female mice, respectively, and activated them with calcium ionophore. The capacity to generate LXA_4 was directly compared to recruited inflammatory PMN from female mice where peritonitis

was induced by the yeast antigen zymosan A. Analysis demonstrated that tissue-PMN had a significantly higher capacity to generate LXA_4 than peritoneal inflammatory PMN (Fig. 10A), as LXA_4 formation was 313 ± 63% and 128% ± 31 % higher in tissue PMN from lacrimal glands and cervical lymph nodes, respectively. The functional upregulation of the LXA_4 circuit in tissue PMN directly correlated with a marked difference in RNA expression of 5-LOX and 15-LOX (Fig. 10B). Expression of 5-LOX was 9 – 21 fold higher in inflammatory PMN compared to tissue PMN while expression of 15-LOX, a marker of leukocyte housekeeping function (16), was 25 – 656 fold higher in tissue PMN than in inflammatory PMN. To determine if T cells are able to respond directly to LXA_4, we assessed expression of LXA_4 receptors ALX (mFPR-rs1 and mFpr-rs2) in isolated naïve $CD3^+$, $CD4^-$ or activated $CD3^+$, $CD4^+$ T cells from draining lymph nodes (Fig. 10C). QPCR analysis demonstrated robust expression of both receptors in T cells and expression of ALX2 (mFpr2, mFPR-rs2) was upregulated 4.4 fold in activated $CD4^+$ T cells. To test the hypothesis that LXA_4 can regulate T cell function *in vivo*, we treated female mice with a combined topically (100 ng, *tid*) and systemic dose (1 μg, *qd*) of LXA_4 for 10 days after initiating dry eye disease (Fig. 10D-F, Fig. S2). Consistent with the hypothesis that reduced levels of LXA_4-producing tissue PMN are a significant factor in CD4 T Cell activation, treatment with LXA_4 significantly inhibited $CD4^+$ T cells in draining lymph nodes by 38 ± 10% (Fig. S2A). Regulation of CD4 T cells by LXA_4 treatment correlated with attenuated dry eye pathogenesis as evidenced by a significant increase in goblet cells and mucin secretion in the conjunctiva (Fig. S2B). To define which $CD4^+$ T cell types are regulated by LXA_4 treatment we quantified T_H1, T_H17 and T_{reg} cells in draining lymph nodes by flow cytometry after 10 days of desiccating stress. LXA_4 treatment almost completely abrogated T_H1 cells as evidenced by by 88 ± 4% decreases and also decreased T_H17 cells by 27 ± 4% (Fig. 10E, 10F). The marked decrease in T effector cells caused by LXA_4 treatment correlated with an increase in T_{reg} cells by 96 ± 22% (Fig. 10D).

Discussion

A key feature of immune-driven aqueous tear deficient dry eye diseases is activation of effector T cells and their autoimmune targeting of the ocular surface and lacrimal gland. The reason why this ocular surface disease has such a high prevalence in females remains poorly defined or is it clear what causes the misguided activation of effector T cells (23, 47, 48). The ability of estrogen and especially testosterone to regulate lacrimal gland function and inflammatory pathway in epithelial cells *in vitro* and *in vivo* implicates sex-steroids as a likely factor in the pathogenesis of dry eye disease in females (47, 49–51). However, limited studies have investigated if there are sex-specific differences in the initiation, regulation or outcome of inflammatory, immune or injury responses in the eye. Employing the established mouse model of desiccating stress that recapitulates key features of effector T cell driven human aqueous tear deficient dry eye disease (20, 26–28), we discovered marked sex-specific differences in ocular surface pathogenesis, activation of effector T cells and Tregs and regulation of a previously unknown LXA_4 producing tissue-PMN population. The standard mouse model of desiccating stress uses scopolamine, a non-specific acetylcholine receptor antagonist, to reduce tear production in the lacrimal gland. A cholinergic-anti-inflammatory pathway has been implicated as a potential counter-regulatory circuit in

inflammatory diseases and nicotinic acetylcholine receptors are expressed in lymphocytes, macrophages and PMN(52). No experiments have addressed if acetylcholine regulates the LXA_4 pathway and explored if scopolamine disrupts that counter-regulatory circuit, which could be a factor in the disease pathogenesis.

In human keratocunjunctivitis sicca infiltration of the lacrimal gland by autoreactive T_H1 and T_H17 cells leads to deficient tear production, which as a downstream effect can cause corneal epithelial defects (20). Despite subjecting matched male and female mice to identical desiccating stress and pharmacological inhibition of lacrimal gland function, we observed subtle but robust increased corneal epithelial defects, decreased number of goblet cells and lower mucin and tear production in females than in males. These findings suggest a female-specific epithelial response to desiccating stress.

Resolution of minor epithelial defects depends on the time course for restoring the epithelial barrier, we have previously demonstrated that acute epithelial wound healing is delayed in female mice in response to repeated mild corneal abrasion injuries (24) or in human female patients treated for corneal fungal ulcers (25). The female-specific wound healing response can be induced in males by activation of the epithelial estrogen receptor ERβ and is mediated in large part by functional down-regulation an epithelial LXA_4 circuit (24). Since epithelial injury response are tightly linked to inflammation, it is important to note that activation of ERβ also reduces recruitment of PMN in the healing cornea. However, these corneal PMN, unlike in most other tissues, drive wound healing and nerve regeneration (7, 9, 10) and thus are critical to the resolution of injury responses. The unusual function of corneal PMN in mild injury responses also suggest that the ocular surface, by yet to be defined factors, promotes or recruits a novel functional phenotype of PMN. It is likely that these regulatory PMN are a significant factor in the female-specific corneal injury response. This hypothesis is strongly supported by our current findings that demonstrate striking sex-specific differences in tissue PMN in the lacrimal gland and draining lymph nodes.

Normal lacrimal glands and draining lymph nodes in females contained 2–4 times as many PMN as matched males. More importantly, desiccating stress triggered an early female and tissue specific PMN response. The most striking sex-specific differences in tissue PMN was observed in draining lymph nodes. Desiccating stress triggered a 2–10 fold increase in male lymph node PMN, which in sharp contrast resulted in a diametric response in females, namely a marked decrease in lymph node PMN that remained depressed throughout the entire dry eye time course. Depressed lymph node PMN number correlated directly with an early and female-specific increase in activated $CD4^+$ effector T cells (T_H1 and T_H17) and a decrease in regulatory T cells (T_{reg}), which suggest that these resident tissue-PMN have a regulatory role in immune-driven dry eye disease.

Immune-driven dry eye pathogenesis has been largely attributed to aberrant activation of T_H1 and T_H17 and impaired suppression of these effector T cells by T_{reg}. However, the mechanism for the misguided activation of autoreactive T cell remains obscure. In view of the important interplay of innate and adaptive immune effector cells in initiating adaptive immune responses, it is likely that dysregulated interaction of effector cells in the ocular surface is a factor in aberrant activation of autoreactive T cells. Recent studies have begun to

explore the role of macrophages in autoimmune dry eye syndrome (53). However, PMN, which are the most abundant innate immune effector cells, have largely been ignored as a significant cell type in the pathogenesis of ocular immune responses. PMN presumed role in the eye is host defense and due to their pro-inflammatory actions are considered downstream and recruited effector cells in inflammatory diseases that cause collateral tissue damage. Hence, our identification of a population of tissue PMN in the limbus, lacrimal gland and cervical draining lymph nodes in normal healthy mice was unexpected. The fact that loss of tissue-PMN by either the female-specific response to desiccating stress or by antibody depletion correlated with amplified effector T cell activation in all ocular tissues strongly implicates tissue-PMN as relevant suppressor cells.

We used independent and established approaches/markers to confirm the identity of tissue-PMN that included cell morphology, MPO activity, the specific Ly6G (clone 1A8) antibody (3), flow cytometry and IHC. The concept of a single primitive PMN cell type has rapidly evolved and distinct populations of PMN-like effector cells have emerged that include myeloid derived suppressor cells, tumor associated neutrophils, B cell-helper neutrophils and suppressor neutrophils (3, 5, 6). Even though there are numerous markers for the emerging PMN populations no single or combined surface markers can clearly identify subpopulation of PMN, especially in mice, and classification is often based on functions (3). The relatively low number of ocular tissue PMN is a hurdle for an extensive surface marker analysis. However, a unique feature of these tissue PMN in the lacrimal gland and cervical lymph nodes of females is their 3–5 fold higher capacity to generate LXA_4 when directly compared to recruited inflammatory PMN. The amplified endogenous formation of LXA_4 by tissue PMN is matched by high expression of 15-LOX and markedly lower expression of 5-LOX. It is important to note that 15-LOX expression is also associated with wound healing and regulatory function in macrophages as it is a differentiation marker of the alternatively activated M2 phenotype but not inflammatory macrophages and is highly expressed in resident tissue macrophages where it has been identified as critical pathway for maintaining immune tolerance (54–56). More importantly, induction of 15-LOX expression induces pro-resolving/anti-inflammatory function in recruited human peripheral blood PMN (16). Multiple lines of evidence in our study provide strong proof of concept that LXA_4-producing tissue PMN have regulatory functions in draining lymph nodes: 1) isolated naïve and $CD4^+$ lymphocytes from draining lymph express ALX receptors, 2) systemic treatment with LXA_4 inhibits activation of T_H1 and T_H17 effector T cells and upregulates T_{reg} cells, 3) endogenous levels of LXA_4 in draining lymph nodes from females directly correlate with PMN numbers and 4) PMN depletion abrogates LXA_4 formation and amplifies effector T cells and downregulates T_{reg} in lymph nodes. The impaired T_{reg} responses in females and their regulation by tissue-PMN are of particular interest as the balance of T_{reg} and effector T cells in regional draining lymph nodes is critical to execute healthy immune responses and avoid aberrant autoimmunity. Impaired T_{reg} suppression of T_H17 cells has been identified as key factor in inducing autoimmune dry eye diseases in mice (44). What factors control T_{reg} numbers and function in lymph nodes is unknown. Hence, our findings that LXA_4 treatment can markedly increase Treg numbers and rescue females from amplified T_H17 and T_H1 driven dry eye disease identifies a novel immune regulatory mechanism. LXA_4 formation in lymph nodes from males, unlike females, did not correlate with changes in PMN numbers.

These findings suggest that in males tissue resident PMN and PMN that are recruited to tissues after initiating desiccating stress likely constitute distinct cell type populations.

The detailed mechanism for LXA_4 regulation of effector or regulatory T cell is of considerable interest and under investigation. However, direct regulation of lymphocytes by LXA_4 is strongly supported by recent reports (18, 57) that demonstrated that innate lymphoid cells, natural killer cells and B cells also express the ALX receptor and are regulated by LXA_4. Several mechanisms have been identified for the direct suppressive activity of PMN that include arginase 1, ROS and MAC1. It is important to note that a primary function and released product of activated PMN are eicosanoids and specific receptors for early response lipid signals are expressed in many lymphocyte populations. A recent study (58) demonstrated that PMN recruitment to lymph nodes after immunization is responsible for the spread of the immune response by producing thromboxane A_2. In addition, LTB_4 another primary product of inflammatory PMN has been established as a key factor in recruiting effector T cells (14, 15). The PMN profile of regulatory eicosanoids likely depends highly on the state of activation or the specific PMN phenotype. We discovered a resident tissue-PMN phenotype that generates LXA_4 in draining lymph nodes and regulates T_H1, T_H17 and T_{reg} responses to ocular surface stress. Sex-specific down-regulation of this resident PMN-LXA_4 circuit identifies a new regulatory system for initiating and preventing aberrant effector T cell activation and subsequent immune-driven ocular surface disease in females.

Supplementary Material

Refer to Web version on PubMed Central for supplementary material.

Acknowledgments

This project was funded in part by the National Institutes of Health Grant (EY022208 and P30EY003176) and the Sjögren's Syndrome Foundation.

Abbreviations used in this article

5-HETE	5-hydroxyeicosatetraenoic acid
5-LOX	5-lipoxygenase
15-HETE	15-hydroxyeicosatetraenoic acid
15-LOX	15-lipoxygenase
ALX	lipoxin A_4 receptor
LC/MS/MS	liquid chromatography-tandem mass spectrometry
LTB_4	leukotriene B_4
LXA_4	lipoxin A_4
MPO	myeloperoxidase
PMN	polymorphonuclear neutrophil

SPM specialized proresolving mediators

References

1. Nathan C. Neutrophils and immunity: challenges and opportunities. Nat Rev Immunol. 2006; 6:173–182. [PubMed: 16498448]
2. Mantovani A, Cassatella MA, Costantini C, Jaillon S. Neutrophils in the activation and regulation of innate and adaptive immunity. Nat Rev Immunol. 2011; 11:519–531. [PubMed: 21785456]
3. Pillay J, Tak T, Kamp VM, Koenderman L. Immune suppression by neutrophils and granulocytic myeloid-derived suppressor cells: similarities and differences. Cell Mol Life Sci. 2013; 70:3813–3827. [PubMed: 23423530]
4. Muller I, Munder M, Kropf P, Hansch GM. Polymorphonuclear neutrophils and T lymphocytes: strange bedfellows or brothers in arms? Trends Immunol. 2009; 30:522–530. [PubMed: 19775938]
5. Puga I, Cols M, Barra CM, He B, Cassis L, Gentile M, Comerma L, Chorny A, Shan M, Xu W, Magri G, Knowles DM, Tam W, Chiu A, Bussel JB, Serrano S, Lorente JA, Bellosillo B, Lloreta J, Juanpere N, Alameda F, Baro T, de Heredia CD, Toran N, Catala A, Torrebadell M, Fortuny C, Cusi V, Carreras C, Diaz GA, Blander JM, Farber CM, Silvestri G, Cunningham-Rundles C, Calvillo M, Dufour C, Notarangelo LD, Lougaris V, Plebani A, Casanova JL, Ganal SC, Diefenbach A, Arostegui JI, Juan M, Yague J, Mahlaoui N, Donadieu J, Chen K, Cerutti A. B cell-helper neutrophils stimulate the diversification and production of immunoglobulin in the marginal zone of the spleen. Nat Immunol. 2012; 13:170–180. [PubMed: 22197976]
6. Cortez-Retamozo V, Etzrodt M, Newton A, Rauch PJ, Chudnovskiy A, Berger C, Ryan RJ, Iwamoto Y, Marinelli B, Gorbatov R, Forghani R, Novobrantseva TI, Koteliansky V, Figueiredo JL, Chen JW, Anderson DG, Nahrendorf M, Swirski FK, Weissleder R, Pittet MJ. Origins of tumor-associated macrophages and neutrophils. Proc Natl Acad Sci U S A. 2012; 109:2491–2496. [PubMed: 22308361]
7. Gronert K, Maheshwari N, Khan N, Hassan IR, Dunn M, Laniado Schwartzman M. A role for the mouse 12/15-lipoxygenase pathway in promoting epithelial wound healing and host defense. J Biol Chem. 2005; 280:15267–15278. [PubMed: 15708862]
8. Li Z, Burns AR, Rumbaut RE, Smith CW. gamma delta T cells are necessary for platelet and neutrophil accumulation in limbal vessels and efficient epithelial repair after corneal abrasion. The American journal of pathology. 2007; 171:838–845. [PubMed: 17675580]
9. Li Z, Burns AR, Smith CW. Two waves of neutrophil emigration in response to corneal epithelial abrasion: distinct adhesion molecule requirements. Investigative ophthalmology & visual science. 2006; 47:1947–1955. [PubMed: 16639002]
10. Li Z, Burns AR, Han L, Rumbaut RE, Smith CW. IL-17 and VEGF are necessary for efficient corneal nerve regeneration. The American journal of pathology. 2011; 178:1106–1116. [PubMed: 21356362]
11. Kenchegowda S, Bazan HE. Significance of lipid mediators in corneal injury and repair. J Lipid Res. 2010; 51:879–891. [PubMed: 19965607]
12. Serhan CN, Chiang N, Van Dyke TE. Resolving inflammation: dual anti-inflammatory and pro-resolution lipid mediators. Nat Rev Immunol. 2008; 8:349–361. [PubMed: 18437155]
13. Funk CD. Prostaglandins and leukotrienes: advances in eicosanoid biology. Science. 2001; 294:1871–1875. [PubMed: 11729303]
14. Tager AM, Bromley SK, Medoff BD, Islam SA, Bercury SD, Friedrich EB, Carafone AD, Gerszten RE, Luster AD. Leukotriene B4 receptor BLT1 mediates early effector T cell recruitment. Nat Immunol. 2003; 4:982–990. [PubMed: 12949531]
15. Goodarzi K, Goodarzi M, Tager AM, Luster AD, von Andrian UH. Leukotriene B4 and BLT1 control cytotoxic effector T cell recruitment to inflamed tissues. Nat Immunol. 2003; 4:965–973. [PubMed: 12949533]
16. Levy BD, Clish CB, Schmidt B, Gronert K, Serhan CN. Lipid mediator class switching during acute inflammation: signals in resolution. Nat Immunol. 2001; 2:612–619. [PubMed: 11429545]

17. Chavis C, Vachier I, Chanez P, Bousquet J, Godard P. 5(S),15(S)-Dihydroxyeicosatetraenoic acid and lipoxin generation in human polymorphonuclear cells: dual specificity of 5-lipoxygenase towards endogenous and exogenous precursors. J Exp Med. 1996; 183:1633–1643. [PubMed: 8666921]
18. Barnig C, Cernadas M, Dutile S, Liu X, Perrella MA, Kazani S, Wechsler ME, Israel E, Levy BD. Lipoxin A4 regulates natural killer cell and type 2 innate lymphoid cell activation in asthma. Sci Transl Med. 2013; 5:174ra126.
19. Niederkorn JY, Stern ME, Pflugfelder SC, De Paiva CS, Corrales RM, Gao J, Siemasko K. Desiccating stress induces T cell-mediated Sjogren's Syndrome-like lacrimal keratoconjunctivitis. J Immunol. 2006; 176:3950–3957. [PubMed: 16547229]
20. Stevenson W, Chauhan SK, Dana R. Dry eye disease: an immune-mediated ocular surface disorder. Arch Ophthalmol. 2012; 130:90–100. [PubMed: 22232476]
21. Stern ME, Schaumburg CS, Pflugfelder SC. Dry eye as a mucosal autoimmune disease. International reviews of immunology. 2013; 32:19–41. [PubMed: 23360156]
22. Schaumberg DA, Dana R, Buring JE, Sullivan DA. Prevalence of dry eye disease among US men: estimates from the Physicians' Health Studies. Arch Ophthalmol. 2009; 127:763–768. [PubMed: 19506195]
23. Schaumberg DA, Sullivan DA, Buring JE, Dana MR. Prevalence of dry eye syndrome among US women. American journal of ophthalmology. 2003; 136:318–326. [PubMed: 12888056]
24. Wang SB, Hu KM, Seamon KJ, Mani V, Chen Y, Gronert K. Estrogen negatively regulates epithelial wound healing and protective lipid mediator circuits in the cornea. FASEB J. 2012; 26:1506–1516. [PubMed: 22186873]
25. Krishnan T, Prajna NV, Gronert K, Oldenburg CE, Ray KJ, Keenan JD, Lietman TM, Acharya NR. Gender differences in re-epithelialisation time in fungal corneal ulcers. Br J Ophthalmol. 2012; 96:137–138. [PubMed: 21979901]
26. Barabino S, Dana MR. Animal models of dry eye: a critical assessment of opportunities and limitations. Invest Ophthalmol Vis Sci. 2004; 45:1641–1646. [PubMed: 15161821]
27. Barabino S, Dana MR. Dry eye syndromes. Chem Immunol Allergy. 2007; 92:176–184. [PubMed: 17264493]
28. Dursun D, Wang M, Monroy D, Li DQ, Lokeshwar BL, Stern ME, Pflugfelder SC. A mouse model of keratoconjunctivitis sicca. Invest Ophthalmol Vis Sci. 2002; 43:632–638. [PubMed: 11867577]
29. Jaeger BN, Donadieu J, Cognet C, Bernat C, Ordonez-Rueda D, Barlogis V, Mahlaoui N, Fenis A, Narni-Mancinelli E, Beaupain B, Bellanne-Chantelot C, Bajenoff M, Malissen B, Malissen M, Vivier E, Ugolini S. Neutrophil depletion impairs natural killer cell maturation, function, and homeostasis. The Journal of experimental medicine. 2012; 209:565–580. [PubMed: 22393124]
30. Daley JM, Thomay AA, Connolly MD, Reichner JS, Albina JE. Use of Ly6G-specific monoclonal antibody to deplete neutrophils in mice. Journal of leukocyte biology. 2008; 83:64–70. [PubMed: 17884993]
31. Biteman B I, Hassan R, Walker E, Leedom AJ, Dunn M, Seta F, Laniado-Schwartzman M, Gronert K. Interdependence of lipoxin A4 and heme-oxygenase in counter-regulating inflammation during corneal wound healing. FASEB J. 2007; 21:2257–2266. [PubMed: 17384141]
32. Leedom AJ, Sullivan AB, Dong B, Lau D, Gronert K. Endogenous LXA4 circuits are determinants of pathological angiogenesis in response to chronic injury. Am J Pathol. 2010; 176:74–84. [PubMed: 20008149]
33. Lemp MA. Report of the National Eye Institute/Industry workshop on Clinical Trials in Dry Eyes. The CLAO journal : official publication of the Contact Lens Association of Ophthalmologists, Inc. 1995; 21:221–232.
34. Research in dry eye: report of the Research Subcommittee of the International Dry Eye WorkShop. The ocular surface. 2007; 5:179–193. [PubMed: 17508121]
35. Bannenberg GL, Chiang N, Ariel A, Arita M, Tjonahen E, Gotlinger KH, Hong S, Serhan CN. Molecular circuits of resolution: formation and actions of resolvins and protectins. J Immunol. 2005; 174:4345–4355. [PubMed: 15778399]

36. Gao Y, Li Z, Hassan N, Mehta P, Burns AR, Tang X, Smith CW. NK cells are necessary for recovery of corneal CD11c+ dendritic cells after epithelial abrasion injury. Journal of leukocyte biology. 2013; 94:343–351. [PubMed: 23695308]
37. Liclican EL, Nguyen V, Sullivan AB, Gronert K. Selective activation of the prostaglandin E2 circuit in chronic injury-induced pathologic angiogenesis. Invest Ophthalmol Vis Sci. 2010; 51:6311–6320. [PubMed: 20610836]
38. Sapieha P, Stahl A, Chen J, Seaward MR, Willett KL, Krah NM, Dennison RJ, Connor KM, Aderman CM, Liclican E, Carughi A, Perelman D, Kanaoka Y, Sangiovanni JP, Gronert K, Smith LE. 5-Lipoxygenase metabolite 4-HDHA is a mediator of the antiangiogenic effect of omega-3 polyunsaturated fatty acids. Sci Transl Med. 2011; 3:69ra12.
39. von Moltke J, Trinidad NJ, Moayeri M, Kintzer AF, Wang SB, van Rooijen N, Brown CR, Krantz BA, Leppla SH, Gronert K, Vance RE. Rapid induction of inflammatory lipid mediators by the inflammasome in vivo. Nature. 2012; 490:107–111. [PubMed: 22902502]
40. Ariel A, Chiang N, Arita M, Petasis NA, Serhan CN. Aspirin-triggered lipoxin A4 and B4 analogs block extracellular signal-regulated kinase-dependent TNF-alpha secretion from human T cells. Journal of Immunology. 2003; 170:6266–6272.
41. El Annan J, Chauhan SK, Ecoiffier T, Zhang Q, Saban DR, Dana R. Characterization of effector T cells in dry eye disease. Investigative ophthalmology & visual science. 2009; 50:3802–3807. [PubMed: 19339740]
42. De Paiva CS, Chotikavanich S, Pangelinan SB, Pitcher JD 3rd, Fang B, Zheng X, Ma P, Farley WJ, Siemasko KF, Niederkorn JY, Stern ME, Li DQ, Pflugfelder SC. IL-17 disrupts corneal barrier following desiccating stress. Mucosal immunology. 2009; 2:243–253. [PubMed: 19242409]
43. Zheng X, de Paiva CS, Li DQ, Farley WJ, Pflugfelder SC. Desiccating stress promotion of Th17 differentiation by ocular surface tissues through a dendritic cell-mediated pathway. Investigative ophthalmology & visual science. 2010; 51:3083–3091. [PubMed: 20130281]
44. Chauhan SK, El Annan J, Ecoiffier T, Goyal S, Zhang Q, Saban DR, Dana R. Autoimmunity in dry eye is due to resistance of Th17 to Treg suppression. Journal of immunology. 2009; 182:1247–1252.
45. Chauhan SK, Dana R. Role of Th17 cells in the immunopathogenesis of dry eye disease. Mucosal immunology. 2009; 2:375–376. [PubMed: 19532120]
46. Li Z, Rumbaut RE, Burns AR, Smith CW. Platelet response to corneal abrasion is necessary for acute inflammation and efficient re-epithelialization. Invest Ophthalmol Vis Sci. 2006; 47:4794–4802. [PubMed: 17065490]
47. Schaumberg DA, Buring JE, Sullivan DA, Dana MR. Hormone replacement therapy and dry eye syndrome. JAMA. 2001; 286:2114–2119. [PubMed: 11694152]
48. Gayton JL. Etiology, prevalence, and treatment of dry eye disease. Clinical ophthalmology (Auckland, NZ). 2009; 3:405–412.
49. Schaumberg DA, Sullivan DA, Dana MR. Epidemiology of dry eye syndrome. Adv Exp Med Biol. 2002; 506:989–998. [PubMed: 12614022]
50. Sullivan DA, Schaumberg DA, Suzuki T, Schirra F, Liu M, Richards S, Sullivan RM, Dana MR, Sullivan BD. Sex steroids, meibomian gland dysfunction and evaporative dry eye in Sjogren's syndrome. Lupus. 2002; 11:667. [PubMed: 12413064]
51. Sullivan DA, Sullivan BD, Evans JE, Schirra F, Yamagami H, Liu M, Richards SM, Suzuki T, Schaumberg DA, Sullivan RM, Dana MR. Androgen deficiency, Meibomian gland dysfunction, and evaporative dry eye. Ann N Y Acad Sci. 2002; 966:211–222. [PubMed: 12114274]
52. de Jonge WJ, Ulloa L. The alpha7 nicotinic acetylcholine receptor as a pharmacological target for inflammation. British journal of pharmacology. 2007; 151:915–929. [PubMed: 17502850]
53. Zhou D, McNamara NA. Macrophages: important players in primary Sjogren's syndrome? Expert review of clinical immunology. 2014; 10:513–520. [PubMed: 24646086]
54. Kuhn H V, O'Donnell B. Inflammation and immune regulation by 12/15-lipoxygenases. Progress in Lipid Research. 2006; 45:334–356. [PubMed: 16678271]

55. Dioszeghy V, Rosas M, Maskrey BH, Colmont C, Topley N, Chaitidis P, Kuhn H, Jones SA, Taylor PR, O'Donnell VB. 12/15-Lipoxygenase regulates the inflammatory response to bacterial products in vivo. J Immunol. 2008; 181:6514–6524. [PubMed: 18941242]

56. Uderhardt S, Herrmann M, Oskolkova OV, Aschermann S, Bicker W, Ipseiz N, Sarter K, Frey B, Rothe T, Voll R, Nimmerjahn F, Bochkov VN, Schett G, Kronke G. 12/15-lipoxygenase orchestrates the clearance of apoptotic cells and maintains immunologic tolerance. Immunity. 2012; 36:834–846. [PubMed: 22503541]

57. Ramon S, Bancos S, Serhan CN, Phipps RP. Lipoxin A(4) modulates adaptive immunity by decreasing memory B-cell responses via an ALX/FPR2-dependent mechanism. Eur J Immunol. 2014; 44:357–369. [PubMed: 24166736]

58. Yang CW, Unanue ER. Neutrophils control the magnitude and spread of the immune response in a thromboxane A2-mediated process. J Exp Med. 2013; 210:375–387. [PubMed: 23337807]

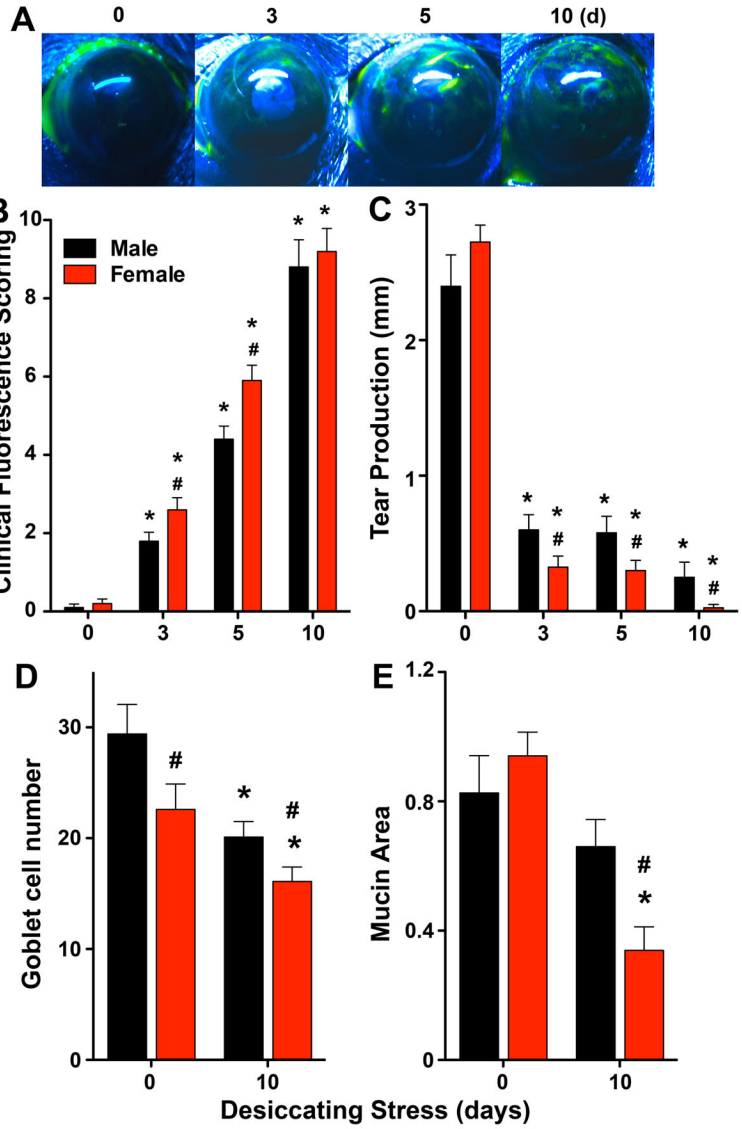

Figure 1. Desiccating stress causes increased ocular surface pathogenesis in females

Age-matched male and female C57BL/6J mice were subjected desiccating stress in a low humidity environmental cubicle (n=10). (A) Images are representative fluorescein-stained corneas from female at each time point. (B) Disease severity (ocular surface lesions) was assessed by clinical fluorescence scoring system. (C) Tear production was measured by Schirmer's test. (D) Sex-specific conjunctival goblet cells were manually counted, and mucin area secreted in conjunctiva was measured by imageJ software from eyelids collected at day 0 (healthy) or 10 days after initiating desiccating stress (n=10). ($^{\#}p<0.05$, females versus males, unpaired *t* test; (B–C)* $p<0.05$, versus sex-specific 0 day, one-way ANOVA; (D–E) *$p<0.05$, healthy versus 10 days desiccating stress).

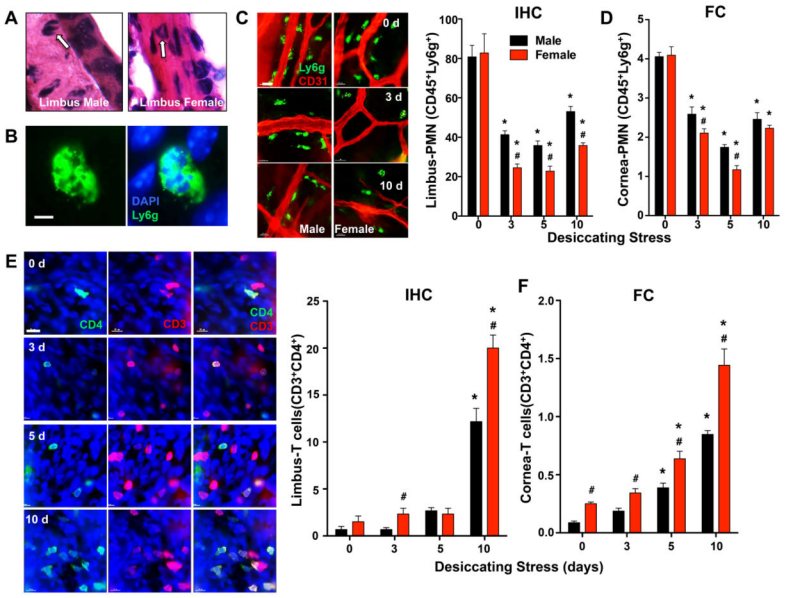

Figure 2. Sex-specific regulation of a tissue-PMN population and CD4+ T cell activation in the corneal limbus

(**A**) Identification of tissue-PMN (arrow) by histology in H&E stained corneal limbus sections. (**B**) Identification of tissue-PMN by IHC with Ly6g (1A8 clone) antibody (green) and DAPI nuclear stain (blue). Scale bars: 10 μm. (**C**) IHC quantification of $CD45^{+}Ly6g^{+}$ PMN in corneas with limbus. The total number of corneal PMN in each of nine, 40× fields of view comprising the diameter of a cornea was counted by IHC quantification. Images are representative whole mount corneas stained for PMN (Ly6g, green) and blood vessels' endothelial cell (CD31, red) markers at day 0 or 3 or 10 days after initiating desiccating stress. Scale bars: 20 μm. (**D**) Frequencies of PMN ($CD45^{high}Ly6g^{high}$) among absolute number of cornea-limbus cells were measured by flow cytometry. (**E**) IHC quantification of $CD3^{high}$ $CD4^{high}$ T cells in corneas with limbus. The total number of corneal $CD3^{high}$ $CD4^{high}$ T cells in each of nine, 40× fields of view comprising the diameter of a cornea was counted by IHC. Images are representative whole mount corneas stained with T cell (CD3, red) and activated T cell (CD4, green) markers in females at day 0 or 3, 5 or 10 days after initiating desiccating stress. Scale bars: 20 μm. (**F**) Frequencies of $CD3^{high}CD4^{high}$ T cells among absolute number of cornea-limbus cells was measured by flow cytometry. (IHC quantification: n=6; FC quantification: 3 independent experiments with 5 pooled corneas for each group; # $p<0.05$, female versus male, unpaired *t* test; * $p<0.05$, compared to sex-specific 0 day, one-way ANOVA.)

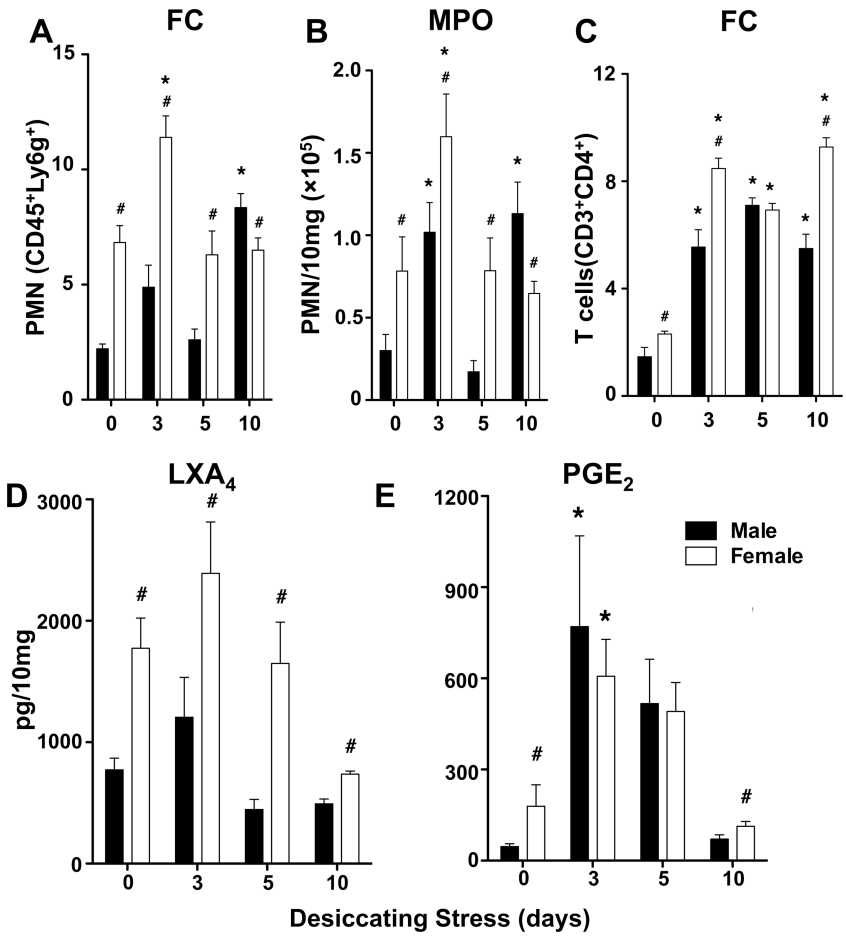

Figure 3. Desiccating stress triggers an amplified PMN and CD4$^+$ T cells response that correlates with sex-specific formation of LXA$_4$ in female lacrimal glands

(A) Quantification of CD45^{high}Ly6g^{high} PMN by flow cytometry (FC): frequencies of PMN (CD45^{high}Ly6g^{high}) among absolute number of cells from lacrimal glands from males and females at 0 or 3, 5 or 10 days after initiating desiccating stress. (**B**) Quantification of lacrimal gland PMN by myeloperoxidase (MPO) activity. PMN numbers were calculated based on peritoneal PMN calibration curves. (**C**) Quantification of CD3^{high}CD4^{high} T cells in lacrimal glands: frequencies of CD3^{high} CD4^{high} T cells among absolute number of cells from lacrimal glands. (**D**) LXA$_4$ and (**E**) PGE$_2$ formation in lacrimal glands was measured in healthy (day 0) and 3, 5 and 10 days after initiating desiccating stress by LC/MS/MS-based lipidomics. Endogenous lipid mediator tissue levels were corrected for recovery of class specific deuterated internal standards and tissue weight. (MPO activity: n=5; FC quantification: 3 independent experiments with 5 pooled lacrimal glands for each group; # p<0.05, female versus male, unpaired t test; * p<0.05, compared to sex-specific 0 day, one-way ANOVA.)

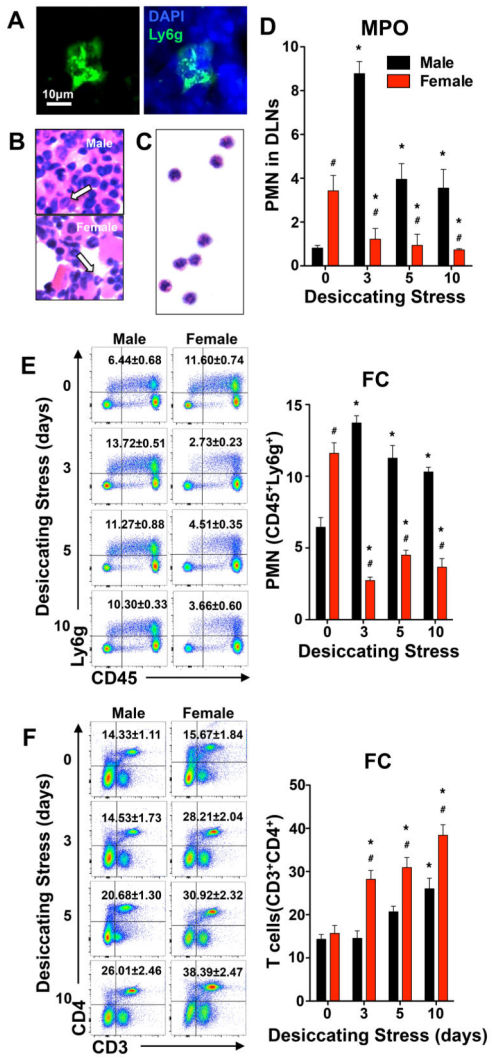

Figure 4. Female-specific regulation of resident PMN and T cell activation in cervical draining lymph nodes

(**A**) PMN identification in inactivated female lymph node sections by IHC. Scale bars: 10 μm. (**B**) Histological identification of PMN in inactivated female lymph nodes sections by H&E staining. (**C**) Isolated H&E stained PMN. PMN from inactivated female draining lymph nodes were negatively isolated by magnetic cell separation and isolation system and stained by H&E. (**D**) Lymph node PMN quantification in males and females by MPO assay. (**E**) Flow cytometry quantification of $CD45^{high}Ly6g^{high}$ PMN. Left panels representative flow cytometry analysis dot plots. Right panel frequencies of PMN ($CD45^{high}Ly6g^{high}$) among absolute number of cells from cervical draining lymph nodes collected at day 0 or 3, 5 or 10 days after initiating desiccating stress. (**F**) Flow cytometry quantification of $CD3^{high}CD4^{high}$ T cells in cervical draining lymph nodes. Left panel, representative flow cytometry analysis dot plots. Right panel, frequencies of $CD3^{high}CD4^{high}$ T cells. (MPO activity: n=5, pooled cervical draining lymph nodes from 1 mouse for each group; FC quantification: n=3 with pooled cervical lymph nodes from 1 mouse for each group; #

$p<0.05$, female versus male, unpaired t test; *$p<0.05$ compared to sex-specific 0 day, one way ANOVA.)

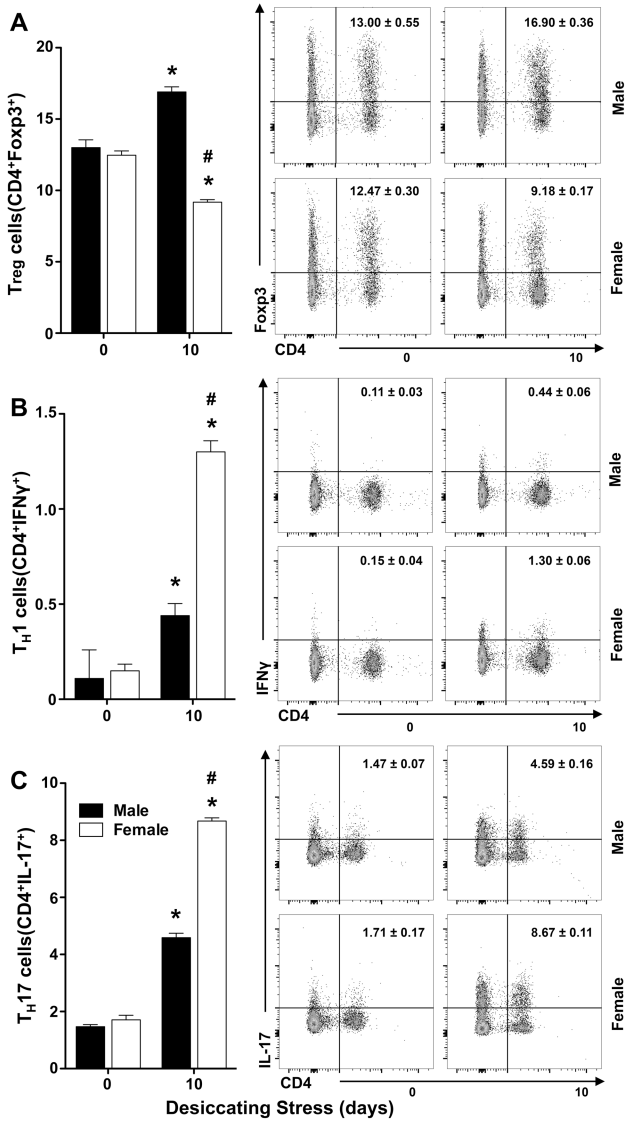

Figure 5. Sex-specific regulation of effector T_H1, T_H17 cells and regulatory T cells (T_{reg}) in cervical draining lymph nodes

(A–C) Left panels flow cytometry quantification: (A) frequencies of T_{reg} cells ($CD4^+Foxp3^+$) among absolute number of lymphocytes from cervical draining lymph nodes collected at day 0 (healthy) or 10 days after initiating desiccating stress, (B) quantification of $CD4^+IFN\gamma^+$ T_H1 cells, (C) quantification of $CD4^+IL17^+$ T_H17 cells. Right panels: representative and respective flow cytometry dot plots. (3 independent experiments with pooled cervical lymph nodes from 1 mouse for each group; # $p<0.05$, females versus males, unpaired *t* test; * $p<0.05$, healthy versus 10 days desiccating stress, unpaired *t* test).

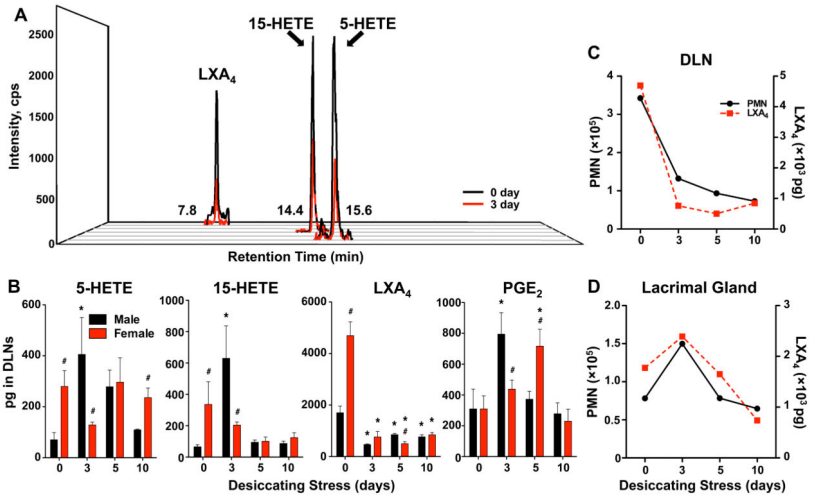

Figure 6. Female-specific changes in the lymph node PMN-LXA_4 circuit during desiccating stress

(**A**) Representative multiple reaction monitoring (MRM) LC/MS/MS chromatogram for 5-HETE, 15-HETE and LXA_4 from female inactivated (0 day, black) cervical lymph nodes and 3 days (red) after initiating desiccating stress. (**B**) LC/MS/MS-based lipidomic quantification of endogenous 5-HETE, 15-HETE, LXA_4, and PGE_2 in cervical draining lymph nodes of males and females. Tissue PMN dependent LXA_4 formation in cervical draining lymph nodes (**C**) and lacrimal glands (**D**) of females. Plotted are the number of PMN (black) and endogenous LXA_4 (red) in pooled lymph nodes and lacrimal glands at 0 and 3, 5 and 10 days after initiating desiccating stress. (n=5, pooled cervical lymph nodes from 1 mouse for each group; $^{\#}$ $p<0.05$, female versus male, unpaired *t* test; * $p<0.05$, compared to sex-specific 0 day, one way ANOVA.)

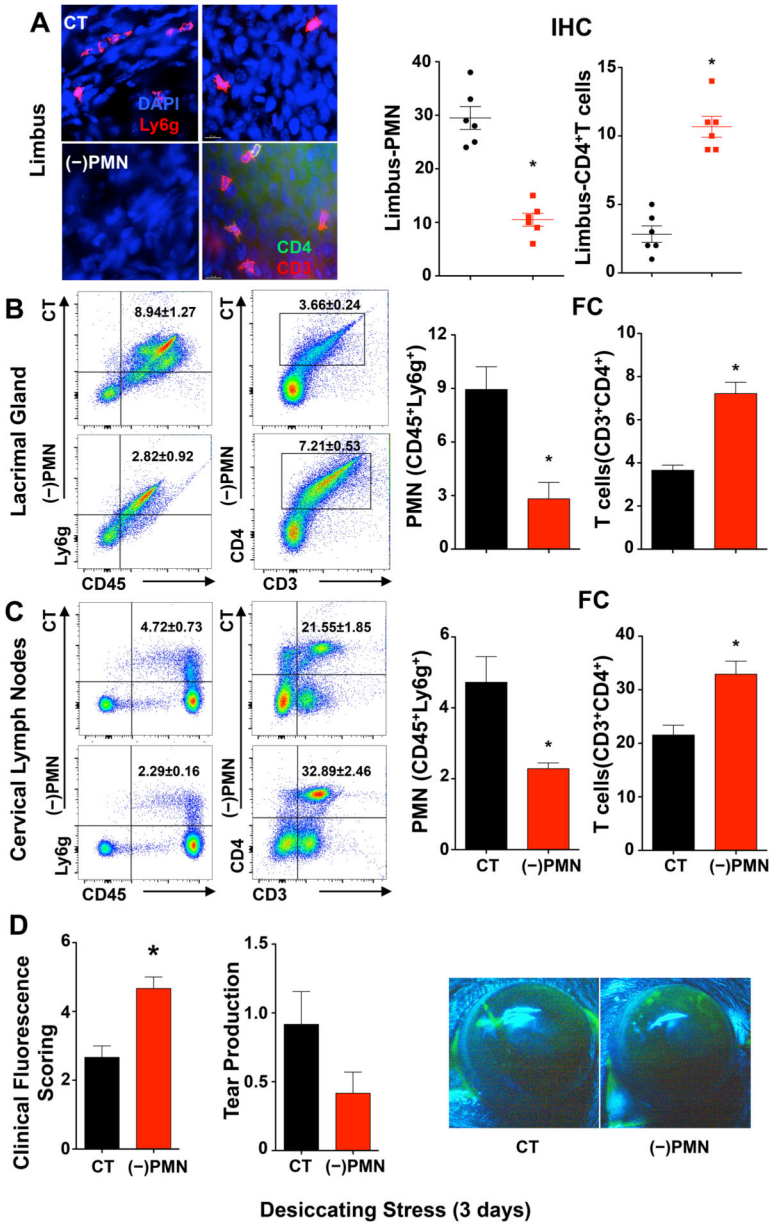

Figure 7. Depletion of Tissue PMN amplifies T cell activation and dry eye pathogenesis

Female mice were injected (i.p.) with PMN-depleting antibodies, purified anti-Ly6g (1A8), (−)PMN, or control IgG (CT) 24 h prior to initiating dry eye disease. (**A**) Quantification of $CD45^{+}Ly6g^{+}$ PMN and $CD4^{+}$ T cells in corneal limbus region after 3 days of desiccating stress. Left panel representative images of IHC. Right panel total number of corneal PMN and $CD4^{+}$ T cells in each of nine 40× fields of view comprising the diameter of a cornea was measured by IHC. Scale bars: 20 μm. (B) Quantification of $CD45^{high}Ly6g^{high}$ PMN and $CD3^{high}CD4^{high}$ T cells in lacrimal glands by flow cytometry. Left panel, representative flow cytometry dot plots. Right panel, frequencies of PMN and $CD4^{+}$ T cells among absolute number of cells from lacrimal glands. (**C**) Quantification of PMN and $CD4^{+}$ T cells in cervical draining lymph nodes by flow cytometry. (D) Corneal epithelial defect was

assessed by clinical fluorescence scoring, and tear production measured by Schirmer's test in females (n=6). Images are representative fluorescein-stained corneas from 3 days dry eye from females treated with IgG control (CT) or PMN depleting antibodies. (IHC quantification: n=6; FC quantification: n=3 with 5 pooled lacrimal glands for each group; * $p<0.05$, compared to control IgG group, unpaired *t* test.)

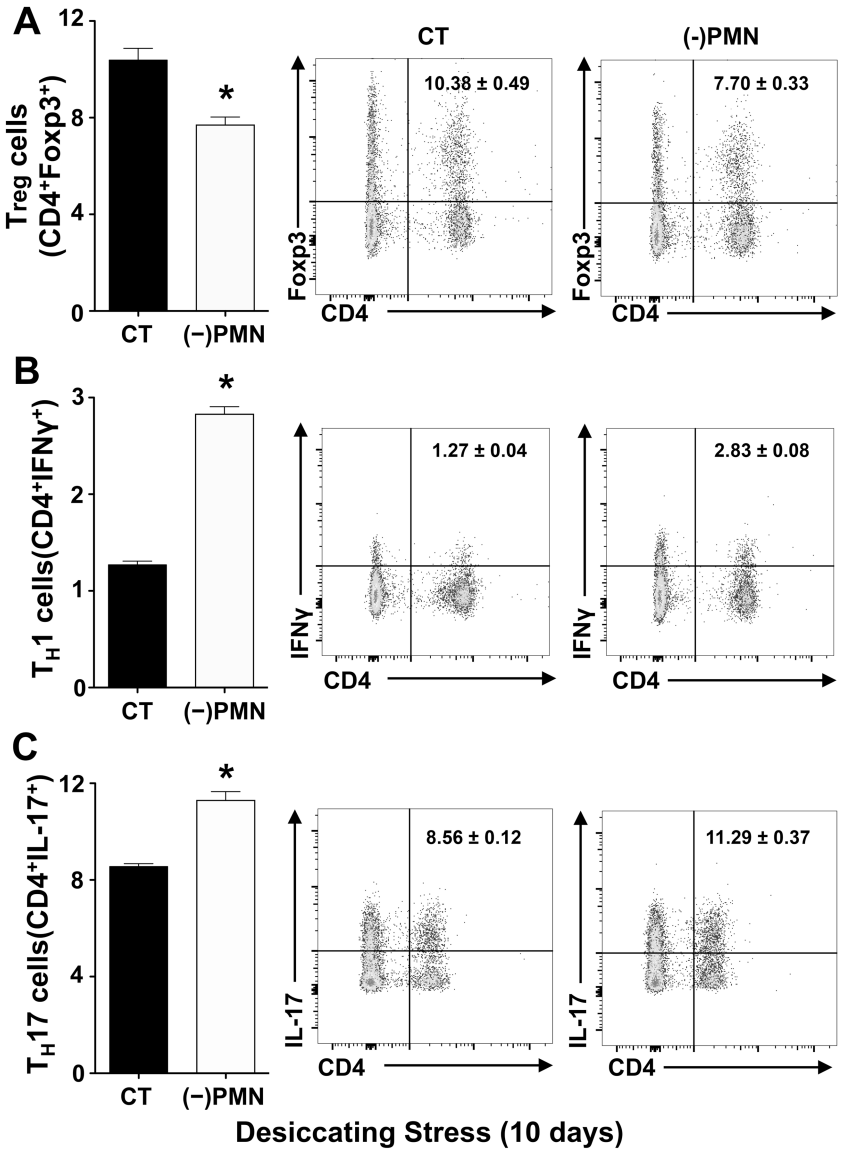

Figure 8. Depletion of tissue-PMN in females amplifies effector T_H1 and T_H17 activation and downregulates T_{reg} cells

PMN were depleted in female mice with purified anti-Ly6g ((-)PMN), and matched control mice were treated with IgG (CT). Treatment was initiated 24h prior to subjecting mice to desiccating stress, and repeated at day 4 and 7 to maintain neutropenia. (A–C) Flow cytometry quantification. Left panels: (A) frequencies of regulatory T cells ($CD4^+Foxp3^+$) among absolute number of lymphocytes from cervical draining lymph nodes collected at day 0 (healthy) or 10 days after initiating desiccating stress, (B) quantification of $CD4^+IFN\gamma^+$ Th1 cells, (C) quantification of $CD4^+IL17^+$ Th17 cells. Right panels: representative and respective flow cytometry dot plots (3 independent experiments with pooled cervical lymph nodes from 1 mouse for each group; * $p<0.05$, compared to control IgG group, unpaired *t* test).

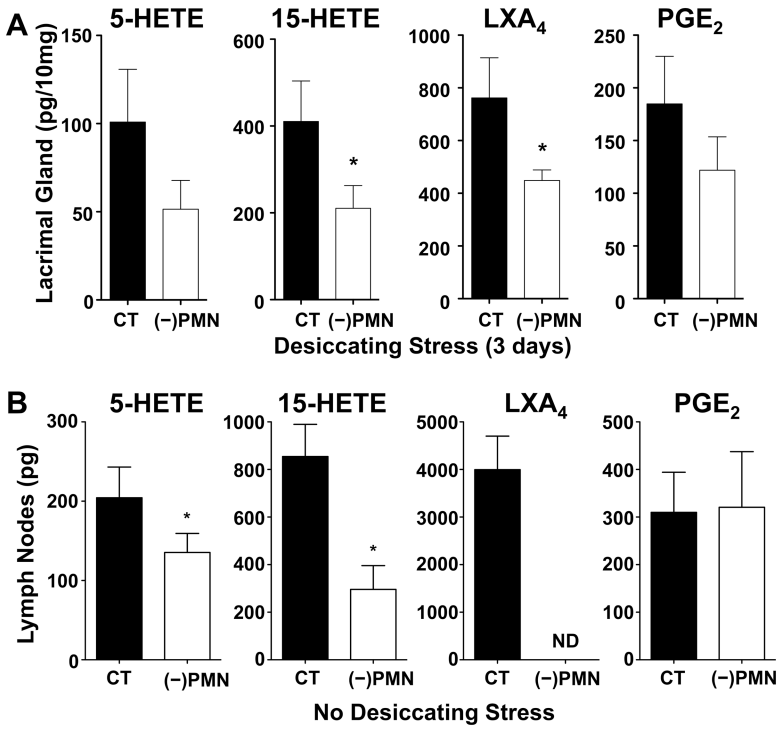

Figure 9. Depletion of tissue PMN in females impairs LXA_4 formation in lymph nodes and lacrimal glands

(**A**) Female mice were injected with PMN-depleting antibodies, purified anti-Ly6g (1A8), or control IgG 24h prior to subjecting mice to 3 days of desiccating stress. LC/MS/MS-based lipidomic quantification of endogenous 5-HETE, 15-HETE, LXA_4 and PGE_2 in lacrimal glands. Lipid mediator tissue levels were corrected by recovery of class specific deuterated internal standards and tissue weight. (**B**) Endogenous 5-HETE, 15-HETE, LXA_4 and PGE_2 levels in cervical draining lymph nodes. Normal female mice were injected with either PMN-depleting antibodies or control IgG 24 h before collection of lymph nodes. (n=5; * $p<0.05$, compared to IgG control, unpaired *t* test.)

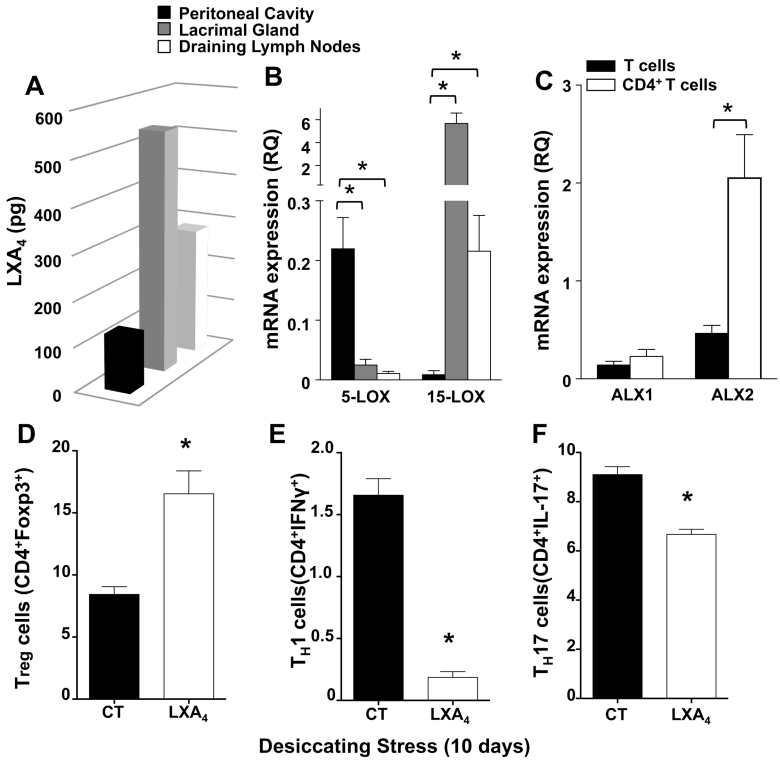

Figure 10. Tissue PMN express an amplified LXA_4 circuit that can regulate lymph node effector and regulatory T cells

(**A**) LC/MS/MS-based quantification of endogenous LXA_4 formation by recruited inflammatory PMN isolated from peritoneal cavity (PC) and tissue PMN isolated from normal female lacrimal glands (LG) and draining lymph nodes (DLN). PMN were activated with calcium ionophore at 37°C for 15 min. LXA_4 formation was normalized to recovery and number of cells (n=5, *pg*/1×10^5 PMN). (**B**) QPCR analysis of 5-LOX and 15-LOX mRNA expression in inflammatory and tissue PMN (**C**) QPCR analysis of LXA_4 receptor (ALX) mRNA expression in isolated naïve $CD4^-$ T cells and activated $CD4^+$ T cells isolated from cervical draining lymph nodes (n=4, * $p<0.05$, compared to peritoneal cavity derived PMN, one way ANOVA). (D–F) Female mice were treated with a combined topical (100 ng, *tid*) and systemic (1 μg, *qd*) LXA_4 dose for 10 days after initiating dry eye disease or PBS alone (CT). (D) Flow cytometry quantification of $CD4^+Foxp3^+$ T_{reg} cells. (E) Flow cytometry quantification of $CD4^+IFN\gamma^+$ T_H1 cells (F) Flow cytometry quantification of $CD4^+IL17^+$ T_H17 cells (n=4; * $p<0.05$, compared to control IgG group, unpaired *t* test).